Traffic 2006; **7:** 903–916
Blackwell Munksgaard

doi: 10.1111/j.1600-0854.2006.00430.x

A Multimeric Membrane Protein Reveals 14-3-3 Isoform Specificity in Forward Transport in Yeast

Kai Michelsen[1], Thomas Mrowiec[1], Karl E. Duderstadt[2], Steffen Frey[1], Daniel L. Minor[2], Matthias P. Mayer[1] and Blanche Schwappach[1,*]

[1]Zentrum für Molekulare Biologie der Universität Heidelberg (ZMBH), Im Neuenheimer Feld 282, D-69120 Heidelberg, Germany
[2]Cardiovascular Research Institute, Departments of Biochemistry and Biophysics and Cellular and Molecular Pharmacology, California Institute for Quantitative Biomedical Research, University of California, San Francisco, 1700 4th Street, San Francisco, CA 94158, USA
**Corresponding author: Blanche Schwappach, b.schwappach@zmbh.uni-heidelberg.de*

Arginine (Arg)-based endoplasmic reticulum (ER) localization signals are sorting motifs involved in the quality control of multimeric membrane proteins. They are distinct from other ER localization signals like the C-terminal di-lysine [-K(X)KXX] signal. The Pmp2p isoproteolipid, a type I yeast membrane protein, reports faithfully on the activity of sorting signals when fused to a tail containing either an Arg-based motif or a -KKXX signal. This reporter reveals that the Arg-based ER localization signals from mammalian Kir6.2 and GB1 proteins are functional in yeast. Thus, the machinery involved in recognition of Arg-based signals is evolutionarily conserved. Multimeric presentation of the Arg-based signal from Kir6.2 on Pmp2p results in forward transport, which requires 14-3-3 proteins encoded in yeast by *BMH1* and *BMH2* in two isoforms. Comparison of a strain without any 14-3-3 proteins (Δ*bmh1*Δ*bmh2*) and the individual Δ*bmh1* or Δ*bmh2* shows that the role of 14-3-3 in the trafficking of this multimeric Pmp2p reporter is isoform-specific. Efficient forward transport requires the presence of Bmh1p. The specific role of Bmh1p is not due to differences in abundance or affinity between the isoforms. Our results imply that 14-3-3 proteins mediate forward transport by a mechanism distinct from simple masking of the Arg-based signal.

Key words: 14-3-3 proteins, Arg-based ER localization signal, forward transport, multimeric membrane protein, yeast

Received 7 February 2006, revised and accepted for publication 22 March 2006, published online 25 May 2006

The cell surface expression of membrane proteins is subject to tight quality control (1). Arginine (Arg)-based ER localization signals are sorting motifs that are involved in the biosynthetic transport of multimeric membrane proteins (2). They occur in polytopic membrane proteins that are subunits of membrane protein complexes. The signal retrieves improperly assembled subunits to the ER until it is inactivated as a result of heteromultimeric assembly. A distinct consensus sequence and their position independence with respect to the distal termini of the protein distinguish Arg-based signals from other ER-sorting motifs. Recent results have lead to a model that links the multimeric state of a membrane protein and, thus, the exposed Arg-based signal to the avidity of 14-3-3 binding, which allows transport of the complex to the cell surface (3). In contrast, monomeric membrane proteins exposing an Arg-based signal are retrieved by coat protein complex I (COPI) (3,4). This model calls for further testing in experiments that require the manipulation of the cellular 14-3-3 pool with respect to copy numbers and isoform composition. To tackle these problems, the yeast *S. cerevisiae* is attractive because the yeast genome encodes for only two 14-3-3 isoforms in contrast to mammalian or plant genomes containing seven or 12 isoforms, respectively. 14-3-3 proteins are ubiquitous, highly conserved dimeric proteins that interact with hundreds of different proteins in diverse eukaryotic signaling pathways. Despite their pervasiveness, the principles underlying the specificity of their protein–protein interactions are only beginning to be uncovered (5–7). Their function in the cell surface trafficking of a number of membrane proteins is well established but mechanistic insight into how they exert this function is scarce (2,8–10).

Results

Pmp2p reports on the activity of Arg-based signals in yeast

In order to find a reporter membrane protein suited to assess the activity of Arg-based signals in yeast, we fused yellow fluorescent protein (YFP) and the C-terminal 36 amino acids of the inwardly rectifying potassium channel Kir6.2 to the yeast membrane protein Pmp2p (Figure 1A). The nonessential *PMP2* gene encodes one of the two 38-residue isoproteolipids affecting the activity of the plasma membrane (PM) proton pump (11). The distal C-terminal tail of Kir6.2 contains an Arg-based ER localization signal (2,12). We followed the subcellular localization of the fusion protein by fluorescence microscopy (Figure 1B). The well-characterized C-terminal di-lysine ER retrieval signal [-K(X)KXX; (13)] was employed as a control sorting motif. A fusion of cyan fluorescent protein (CFP) to histone 2B (*HTB1*) was integrated into the genome of the yeast strain in order to mark the nucleus. Like the -KKTN signal derived from the cytoplasmic tail of the oligosyl-

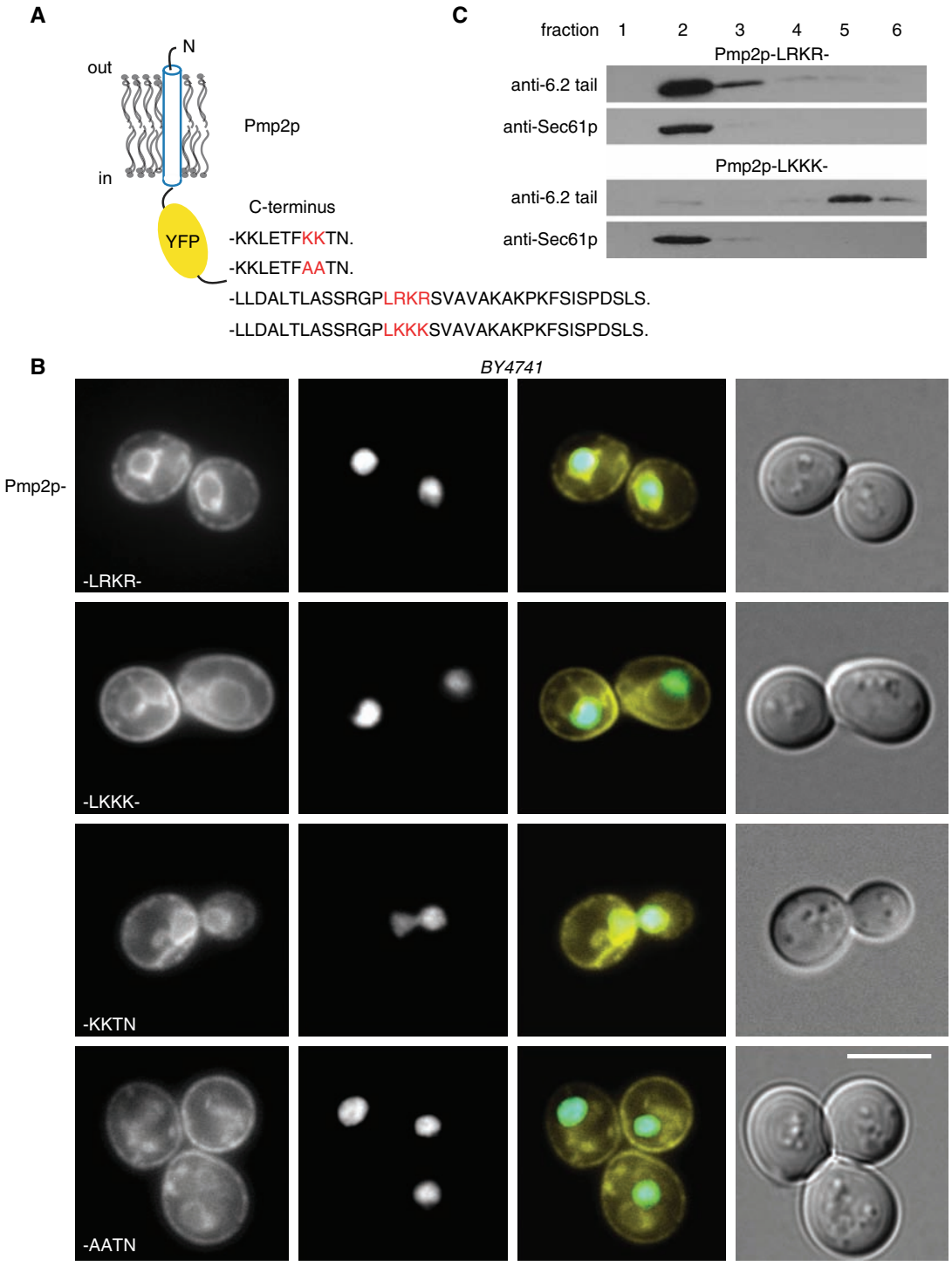

Figure 1: Pmp2p is suited as a membrane reporter protein for peptide sorting motifs in yeast. (A) Schematic representation of Pmp2p fusions to fluorescent proteins (YFP) and C-terminal tails containing active or inactive variants of -KKXX or Arg-based sorting signals. (B) Live cells (strain BY4741; Table 1) expressing the indicated constructs from a *CEN* plasmid were viewed under a fluorescence microscope and pictures were taken integrating over the same period of time. A fusion of CFP to histone 2B (*HTB1*) was integrated into the genome of the strain in order to mark the nucleus. YFP fluorescence images (left) are paired with the corresponding field viewed through a CFP filter and using Nomarski optics (scale bar, 5 μm). (C) Subcellular fractionation on a step sucrose gradient. The six fractions were collected, total protein was precipitated, and loaded from the top to bottom fractions (1–6). The distribution of variants of Pmp2p and the ER marker protein Sec61p was analyzed by immunodetection. The method has been shown to achieve a good separation of ER (fractions 2 and 3) and PM (fractions 5 and 6) (36).

transferase Wbp1p, the tail of Kir6.2 containing the Arg-based signal localized the reporter fusion to the ER as indicated by perinuclear and subcortical fluorescence. Inactivating either sorting motif by mutating the critical residues to alanines or lysines (-AATN instead of -KKTN, -LKKK- instead of -LRKR- in the tail of Kir6.2) resulted in sorting of the reporter fusion to the cell surface and the vacuole (Figure 1B). We confirmed the localization of Pmp2p-LRKR to the ER by subcellular fractionation on sucrose step gradients (Figure 1C). The reporter fusion cofractionated with a marker protein of the ER (Sec61p). Mutating the arginines of the Arg-based signal to lysines has been shown to inactivate the signal (12). Consistently, we observed the reporter in the bottom fractions of the gradient known to contain the PM fraction (14) and devoid of the ER marker when this mutation was introduced into the Pmp2p-GFP reporter fusion (Figure 1C). We conclude that Pmp2p is a reporter protein ideally suited to monitor the activity of Arg-based signals in yeast.

Arg-based ER localization signals have been identified in mammalian membrane proteins of different topology where they mediate the transient ER localization of one or more subunits (2). Eventually, the signal is masked as a result of heteromultimeric assembly. No yeast homologues of these protein complexes exist and, so far, no endogenous yeast membrane protein is known to localize by the exposure of an Arg-based signal. Thus, we wanted to further corroborate that recognition of this sorting motif is, indeed, conserved between yeast and mammals. A unique consensus sequence distinguishes this sorting motif from other ER localization motifs like the -K(X)KXX signal (2). In particular, lysines are incapable of replacing the arginines in the context of this signal. Thus, we investigated several variants of the signal (Figure 2) that have been studied in the context of the Kir6.2 ion channel (12). Next to exclusive ER localization (displayed by reporter fusions -LRKRS-, -LRRRS-) and complete trafficking to the vacuole and cell surface (-AAAAS- and -LKKKS-), we observed intermediate phenotypes: either we detected some forward trafficking in addition to robust ER localization of the bulk of the reporter (-ARKRS-, -LRIRS-, -LRKRA-) or we observed forward trafficking to the vacuole with some residual ER localization (-LRERS-). These phenotypes were fully consistent with the characterization of the signal variants in full-length Kir6.2 (12) and match the results of a random screen in mammalian cells to characterize signal consensus (15). To further test the generality of this finding, we extended our analysis to the Arg-based signal found in the $GABA_B$ subunit GB1 (16). Fusion to the GB1 C-terminus containing the active Arg-based signal (-RSRR-) resulted in ER localization of Pmp2p whereas an inactive, mutated variant [-NSNN-; (16)] of the signal resulted in trafficking of the reporter fusion to the vacuole (Figure 3). We conclude that Arg-based signals from two unrelated mammalian membrane proteins function as ER sorting signals when transferred to the Pmp2p reporter protein. This suggests that the machinery involved in the recognition of Arg-based signals is evolutionarily conserved between yeast, *Xenopus* frog, and mammals.

Multimerization alters the trafficking of the Pmp2p-LRKR reporter

Working with the monomeric reporter protein CD4, the dimeric reporter protein CD8 and a tetramerized variant of CD4 in mammalian cells, we have recently found a correlation between the multimerization state of membrane proteins, binding of dimeric 14-3-3 proteins and forward trafficking (3). In contrast to mammalian cells (seven 14-3-3 isoforms), the yeast genome contains only two genes encoding for 14-3-3 proteins, *BMH1* and *BMH2*. Single knockouts of either gene are viable whereas the double knockout strain is only viable in a specific genetic background [Σ1278b; (17)]. Therefore, the manipulation of 14-3-3 copy numbers and isoform composition is more feasible in yeast than in mammalian cells. To test whether the correlation between multimerization and 14-3-3-dependent forward trafficking is conserved in yeast, we tetramerized the Pmp2p-LRKR reporter protein (Figure 4A) employing the tetramerizing *GCN4* leucine zipper variant pLI (18) in analogy to our tetrameric version of the mammalian CD4 reporter (3) and expressed this green fluorescent protein (GFP) fusion in wildtype (wt) yeast (Figure 4B). The tetrameric Pmp2p-cc-LRKR (-cc- denotes the coiled-coil forming domain, pLI) localized prominently to the vacuole with very weak ER localization still detectable in most cells. Sorting to the vacuole is often considered as the default forward-trafficking route in yeast (19). We did not further investigate why Pmp2p reporter proteins exposing certain inactive variants of the Arg-based signal localized to the PM as well as the vacuolar membrane (Figure 2) and generally considered localization to either compartment as the net result of efficient ER exit and lack of ER retrieval. The residual ER localization observed for Pmp2p-cc-LRKR was due to the presence of the Arg-based signal since the tetramerized Pmp2p reporter exposing the inactive -LKKK- variant of the Arg-based signal [(12); Figures 1 and 2] was not detectable in the ER (Figure 4). The loss of ER localization in Pmp2p-cc-LRKR is most likely not due to a general steric problem that prevents the COPI coat complex from binding to the tail of the reporter protein since the tetrameric Pmp2p-cc-KKTN exposing a C-terminal di-lysine signal still localized to the ER (Figure 4B). The tetramerized tail of Kir6.2 binds 14-3-3 proteins with high avidity, in contrast to a single copy of the same tail (3). Based on this correlation between 14-3-3 binding and forward trafficking of tetramerized CD4 in mammalian cells, we proposed that 14-3-3 proteins can shield the Arg-based signal from the COPI coat and, thereby couple assembly state to forward trafficking. The result that tetrameric Pmp2p-cc-LRKR but not Pmp2p-cc-KKTN leaves the yeast ER suggests that recognition of multiple copies of an LRKR-containing tail by 14-3-3 is conserved in yeast as is the recognition of the monomeric Arg-based signal as an ER localization signal. Next, we directly tested the involvement of 14-3-3

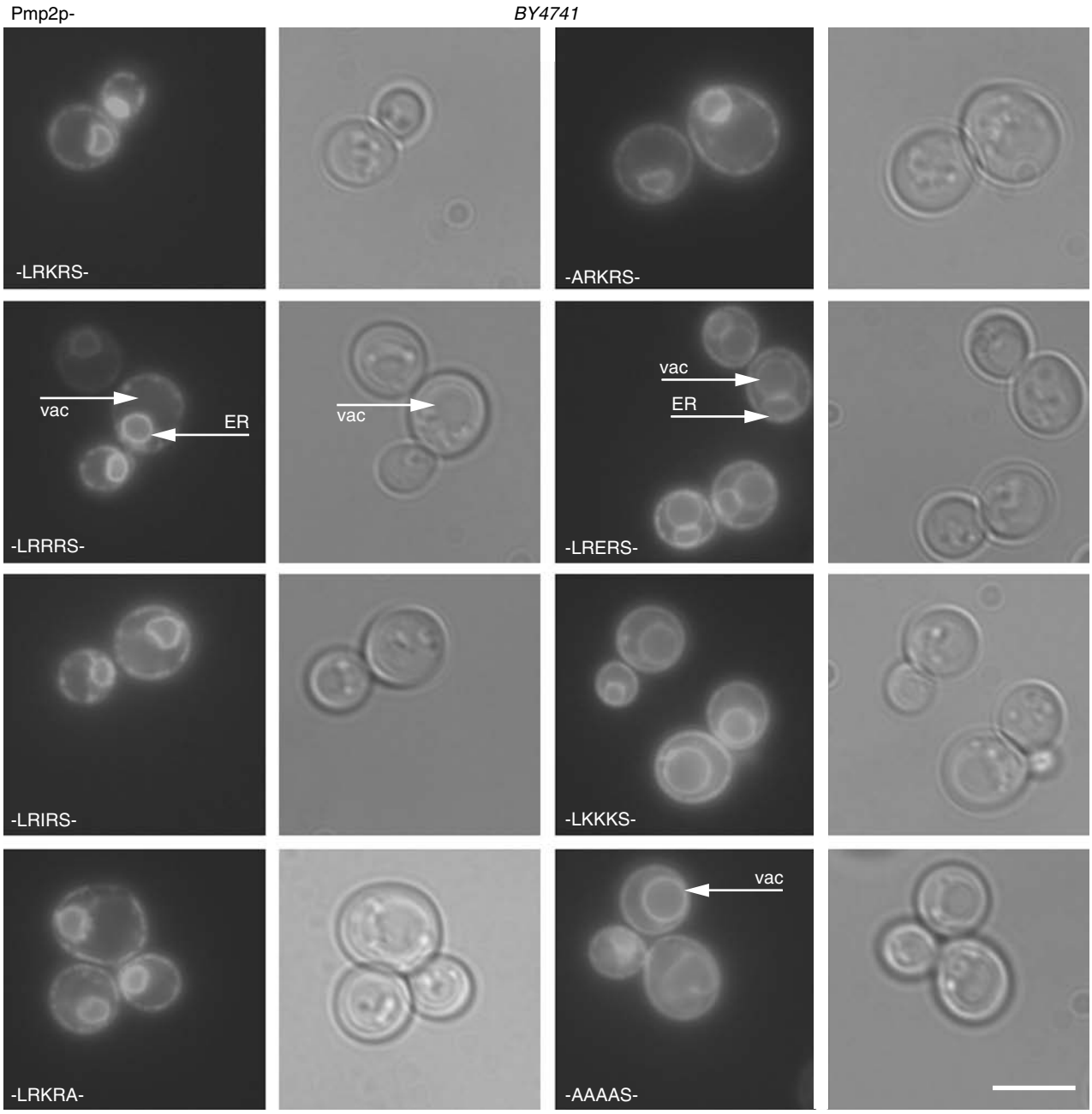

Figure 2: Variants of the Arg-based sorting signal display intermediate sorting efficacies equivalent to the behavior of the same variants in higher eukaryotic cells. Live cells (BY4741; Table 1) expressing the indicated constructs as GFP fusion proteins from a *CEN* plasmid were viewed under a fluorescence microscope and pictures were taken integrating over the same period of time. GFP fluorescence images (top) are paired with the corresponding field photographed using Nomarski optics (scale bar, 5 μm). White arrows indicate the perinuclear ER (ER) or the vacuole (vac).

proteins in the forward trafficking of tetrameric Pmp2p-cc-LRKR.

Absence of 14-3-3 impairs forward trafficking of Pmp2p-cc-LRKR

First, we immunoprecipitated the monomeric and tetrameric Pmp2p reporter proteins fused to the tail of Kir6.2 and tested the corresponding immunoprecipitates for the presence of 14-3-3 proteins (Figure 5). Three independent experiments showed that both Bmh1p and Bmh2p are enriched more than two fold when immunoprecipitates of the tetrameric reporter fusion were compared to those obtained employing the monomer (Figure 5A,B). Since 14-3-3 proteins exist as homo- and heterodimers, we addressed binding of either isoform to the tetrameric reporter protein in the individual deletion mutants by

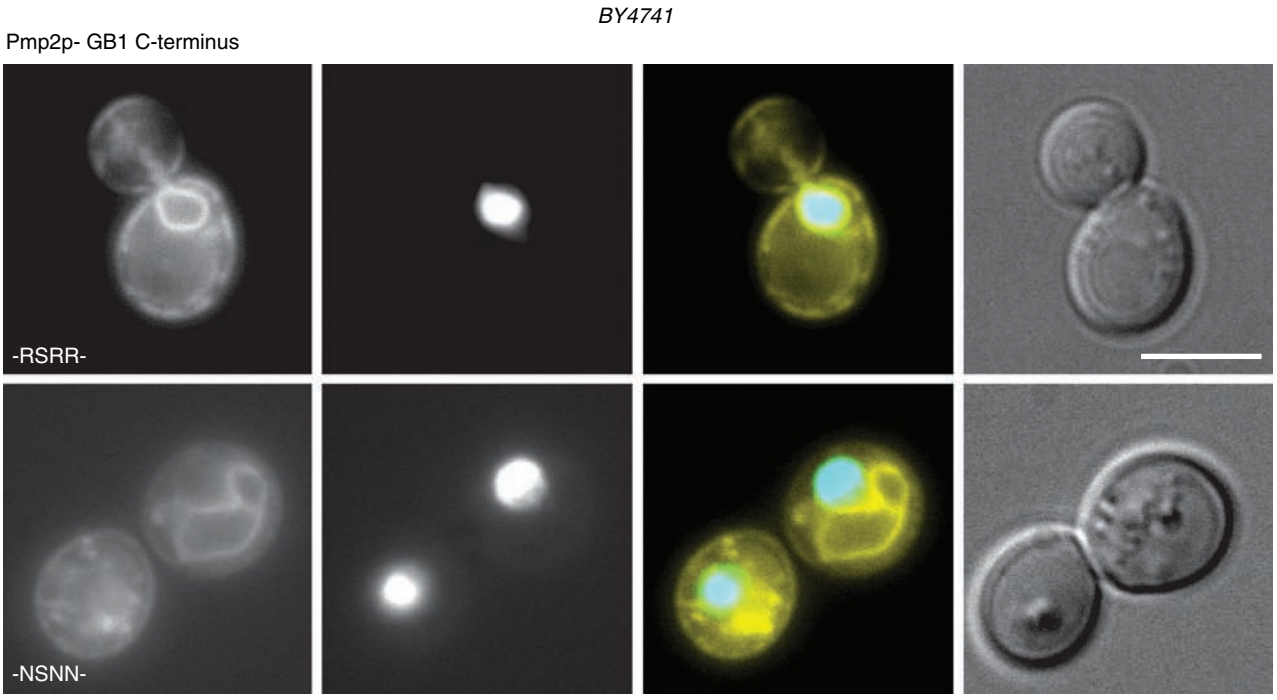

Figure 3: The Arg-based signal present in the C-terminus of the $GABA_B$ receptor subunit GB1 is active in yeast. Details as described in the legend for Figure 1 (scale bar, 5 μm).

coimmunoprecipitation (Figure 5C). These experiments showed that homodimers of Bmh1p or Bmh2p were capable of binding to the tetrameric Kir6.2 tail (see also Figure S1A).

Since Pmp2p-cc-LRKR is able to leave the ER, we wanted to investigate the sorting of this reporter in the absence of any cellular 14-3-3 proteins. Loss of both isoforms is lethal in commonly used laboratory strains of *S. cerevisiae* but is tolerated in the genetic background of strain Σ1278b (17). We transformed this double-deletion and the corresponding wildtype strain with the constructs encoding the monomeric Pmp2p-LRKR or the inactive lysine mutant, and the tetrameric Pmp2p-cc-LRKR or the inactive lysine mutant (Figure 6 and S2). Steady-state ER localization of the monomeric Pmp2p-LRKR reporter was not affected and mutated Pmp2p-LKKK (monomer or tetramer) reached the cell surface and vacuole efficiently in the △*bmh1*△*bmh2* double deletion strain (Figure S2). This suggests that gross function of the secretory pathway is normal in the absence of both 14-3-3 proteins. In contrast to the isogenic wildtype strain, we observed that a significant portion of the tetrameric Pmp2p-LRKR still localized to the ER [as marked by a fluorescent dye specifically accumulating in the ER (20)] in the △*bmh1*△*bmh2* double-deletion strain (Figure 6). The corresponding tetrameric Pmp2p-cc-LKKK mutant was completely localized to the vacuole (Figure S2), which argues against a general forward trafficking defect in the 14-3-3 double-deletion strain. We conclude that 14-3-3 proteins participate in forward trafficking of the tetrameric reporter Pmp2p-cc-LRKR in yeast. Thus, the Pmp2p reporter protein allows us to reconstitute in yeast both phenomena that have been associated with the Arg-based sorting signal: ER localization of monomeric membrane proteins and coupling of the assembly state of a membrane protein to forward trafficking as a result of 14-3-3 recruitment.

Bmh1p controls forward trafficking of the tetrameric Pmp2p-cc-LRKR

The role of different 14-3-3 isoforms in distinct pathways is a fundamental biological problem given the large number of interactions that these proteins engage in. We investigated the phenotype of the individual 14-3-3 knockout strains from the EUROFAN systematic gene deletion project (21) in order to assess the contribution of either isoform to the forward trafficking of the YFP variant of Pmp2p-cc-LRKR (Figure 7A). We imaged cells of the isogenic wt, △*bmh1*, or △*bmh2* deletions strains in several double-blind sessions. A fusion of CFP to histone 2B (*HTB1*) was integrated into the genome of each strain in order to mark the nucleus. This marker allowed unambiguous identification of the perinuclear staining pattern indicative of ER localization. Whilst the steady state localization of Pmp2p-cc-LRKR in the △*bmh2* deletion strain showed even more consistent vacuolar staining than in the wt strain, the △*bmh1* deletion strain showed strong ER localization of the reporter in addition to some weak vacuolar staining (Figure 7A). This phenotype was very

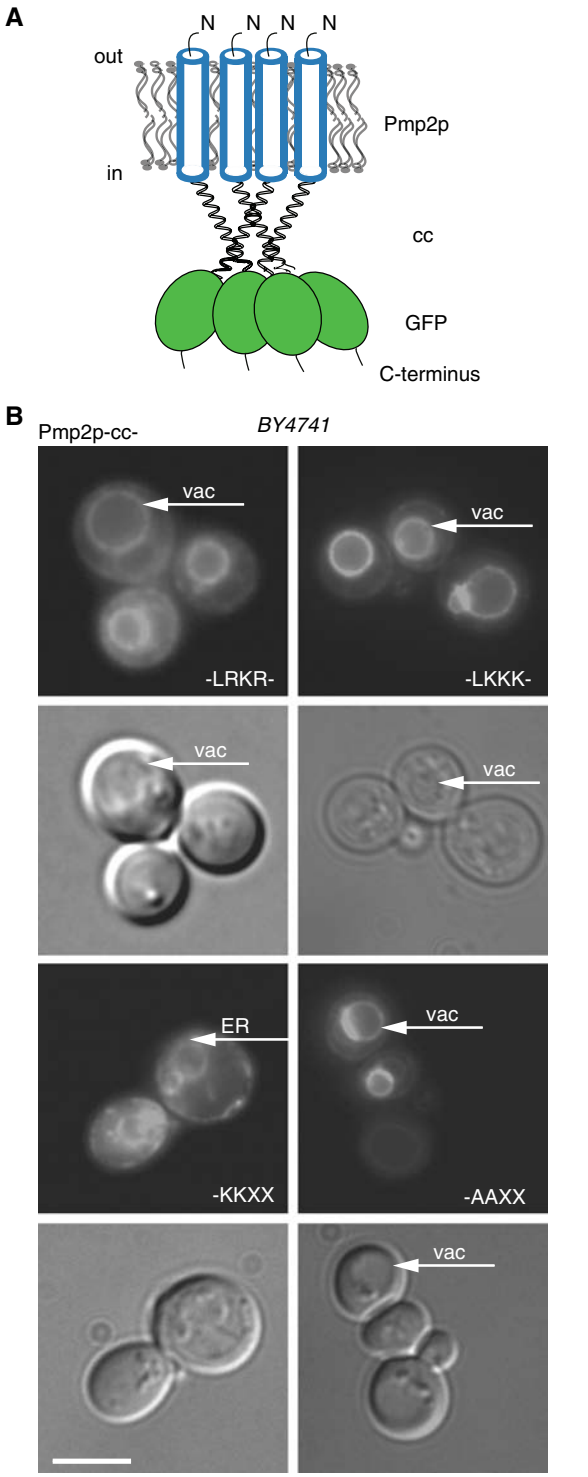

Figure 4: The tetrameric Pmp2p-cc-LRKR reporter leaves the ER efficiently. (A) Schematic representation of the tetrameric Pmp2p reporter. (B) Live wildtype cells (BY4741, Table 1) expressing the indicated GFP fusion constructs from a *CEN* plasmid were viewed under a fluorescence microscope and pictures were taken integrating over the same period of time. GFP fluorescence images (top) are paired with the corresponding field photographed using Nomarski optics (scale bar, 5 μm). White arrows indicate the perinuclear ER (ER) or the vacuole (vac).

similar to what we observed for the double deletion strain (Figure 6) in the genetic background of Σ1278b. The tetrameric Pmp2p-cc-LKKK reporter bearing an inactive Arg-based signal robustly localized to the vacuole in all three strains (Figure 7B). This shows that neither strain displays a general defect in forward trafficking of the tetrameric reporter *per se* to the vacuole. We conclude that Bmh1p but not Bmh2p affects the sorting of the tetrameric Pmp2p-cc-LRKR *in vivo*. Our result suggests isoform specificity of 14-3-3 proteins in the recognition of the Arg-based ER localization signal present in Kir6.2. Alternatively, the isoforms differ in their capacity to mediate the downstream events that eventually alter the localization of the reporter protein.

Bmh1p is present at a three-fold higher copy-number per cell than Bmh2p as has been determined in a global analysis of protein expression in yeast (22). The copy numbers reported for the respective TAP-fusion proteins were 158 000 per cell (Bmh1p) and 47 600 per cell (Bmh2p). Thus, losing Bmh1p has a more drastic effect on the total population of 14-3-3 proteins than losing Bmh2p. The apparent isoform specificity observed *in vivo* could simply be due to the different copy numbers in which the two isoforms are present. To confirm the results obtained using TAP-fusion proteins, we expressed Bmh1p and Bmh2p as untagged proteins and purified them from *E. coli* (Figure S1A). Then we used a polyclonal antiserum (23) that recognizes both isoforms to determine the copy numbers for the two endogenous, unmodified 14-3-3 isoforms in wildtype, △*bmh1*, and △*bmh2* strains by quantitative Western blotting (Figure S1C, D). The signal obtained from total protein extracts isolated from 10^6 yeast cells was compared to calibration curves based on defined amounts of purified Bmh1p and Bmh2p. The resulting numbers were well comparable to those obtained by (22), e.g. 133 000 (±16 000; SEM; $n = 4$) copies per cell for Bmh1p and 58 000 (±19 000; SEM; $n = 3$) copies per cell for Bmh2p. The copy number per cell of one isoform was up-regulated in the respective deletion strain devoid of the other isoform: 214 000 (±22 000; SEM; $n = 4$) copies per cell for Bmh1p in the △*bmh2* strain and 93 000 (±1900; SEM; $n = 2$) copies per cell for Bmh2p in the △*bmh1* strain (Figure S1C, D).

To test the impact of a change in 14-3-3 copy numbers *in vivo*, we over-expressed Bmh2p by integrating one copy of the corresponding gene under the control of the *MET25* promoter in the genome of the △*bmh1* deletion strain to raise the copy number of Bmh2p to approximately 261 000 (±9600; SEM; $n = 8$) per cell (Figure 8). Interestingly, under these conditions the tetrameric Pmp2p-cc-LRKR reporter accumulated in the ER as observed for the △*bmh1* deletion strain. We conclude that, independently from their copy numbers, Bmh1p and Bmh2p play different roles in the forward transport of the multimeric reporter exposing an Arg-based ER localization signal and that Bmh1p was the relevant 14-3-3 protein *in vivo*.

Both yeast 14-3-3 proteins bind the tetrameric Kir6.2 tail with high affinity as demonstrated by coimmunoprecipitation (Figure 5) and affinity purification on a column with immobilized protein A-cc-LRKR tail (Figure S1A). To find out whether quantitative differences in their respective binding affinities could explain their distinct behavior *in vivo*, we set out to determine the pertinent binding parameters quantitatively. Since Bmh2p was the nonfunctional isoform *in vivo* we first used isothermal titration calorimetry (ITC) to compare binding of Bmh2p to the monomeric and the tetrameric Kir6.2 tail. Binding to the monomer was low-affinity since we were not able to observe binding in the concentration range tested. In the same concentration range, binding to the tetramer was well detectable (Figure 9A). The signal could be fitted by a one-to-one-binding curve that yielded a dissociation constant of 6.2 nM. Second, we measured binding of Bmh2p to the tetrameric Kir6.2 tail employing surface plasmon resonance (Figure 9B). The tetrameric protein A-cc-LRKR tail was immobilized on the Biacore chip by chemical cross-linking. Again, the set of binding curves could be fitted based on a one-to-one binding model. The fit gave a dissociation constant of 17.4 nM (±0.8 nM; SEM) for Bmh2p binding to the tetramer. Since the different methods resulted in similar values for the dissociation constant we conclude that either method is suited to investigate the binding of 14-3-3 proteins to the multimeric Kir6.2 tail. Next, we compared the binding of Bmh1p to the data obtained for Bmh2p and obtained a dissociation constant of 13.8 nM (±1.2; SEM) as compared to 17.4 nM (±0.8 nM; SEM) for Bmh2p. We conclude that the differences in affinity between Bmh1p and Bmh2p for the tetrameric LRKR-tail are too small to account for the differences observed in their *in-vivo* capacity to promote forward trafficking of the Pmp2p-cc-LRKR reporter.

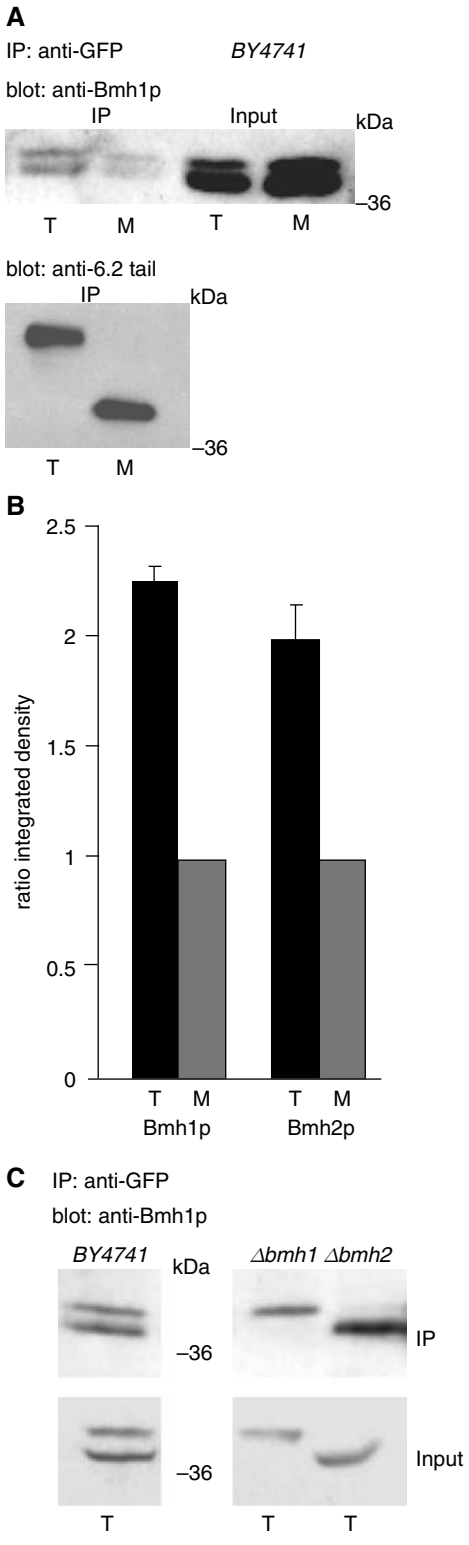

Figure 5: 14-3-3 proteins bind the tetrameric Pmp2p-cc-LRKR reporter with higher avidity than the corresponding monomer. (A) Coimmunoprecipitates obtained by immunoprecipitation of the tetrameric (T) or monomeric (M) Pmp2p reporter fused to the tail of Kir6.2. Anti-Bmh1p blot identifies coimmunoprecipitated 14-3-3 proteins, 2% of the input is shown to demonstrate equal amounts of 14-3-3 proteins in the cellular lysates. Anti-Kir6.2-tail blot controls for comparable enrichment of the two reporter membrane proteins. (B) Densitometric analysis of three independent experiments of which the blots shown in (A) are representative. Values are normalized to the signals obtained for the monomer. (C) Coimmunoprecipitates obtained by immunoprecipitation of the tetrameric (T) from lysates of the individual 14-3-3 deletion strains. Anti-Bmh1p blot identifies the 14-3-3 proteins coimmunoprecipitated with the membrane protein.

Discussion

We established the use of the yeast membrane protein Pmp2p as a reporter that allows monitoring the activity of sorting signals by microscopy. The CD4 and CD8 cell surface glycoproteins are examples for such reporter proteins in mammalian cells but are not useful to study trafficking in the secretory pathway of *S. cerevisiae* because they do not mature normally in yeast (24). Studies of protein sorting motifs in yeast have employed the G-protein coupled

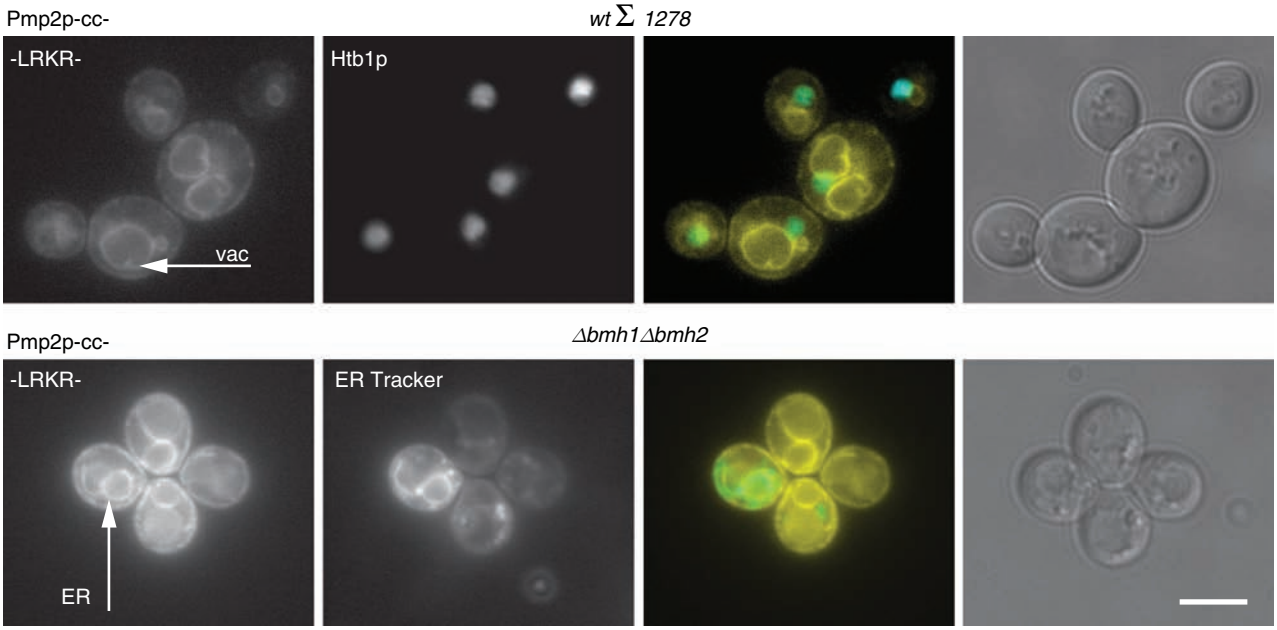

Figure 6: A portion of the tetrameric Pmp2p-cc-LRKR reporter accumulates in the ER in the absence of cellular 14-3-3 proteins. Live cells of the respective genetic background (see Table 1 for full genotypes) expressing the indicated YFP fusion constructs from a *CEN* plasmid were viewed under a fluorescence microscope and pictures were taken integrating over the same period of time. YFP fluorescence images (top) are paired with the corresponding field viewed through a CFP filter (Htb1p-CFP fusion to mark the nucleus for the upper panels and ER-Tracker dye DPX to mark the ER for the lower panels) and by Nomarski optics (scale bar, 5 μm). White arrows indicate the perinuclear ER (ER) or the vacuole (vac).

receptor Ste2p (25) as a reporter in growth assays but Ste2p is known to oligomerize (26,27), which limits its usefulness for studying Arg-based signals (Hebao Yuan and Blanche Schwappach; unpublished results). The isoproteolipid Pmp2p is normally expressed at the cell surface and reports faithfully on the activity of the well characterized -KKXX-COOH signal (Figure 1). Use of this reporter shows that Arg-based signals do indeed function as ER localization signals in yeast. Thus, the machinery involved in recognizing these peptide-sorting motifs is evolutionarily conserved. Previous work had shown that a tail containing an Arg-based signal can reduce the cell surface expression of a heterologous membrane protein in yeast (12). Yet, the functional complementation assay employed to show this did not supply any information on the mechanism by which cell surface expression was reduced. The results presented here do not only demonstrate that the Arg-based signal present in Kir6.2 redirects the reporter to the ER in *S. cerevisiae* but reveal that sequence variants of the signal display similar changes in activity in yeast as observed in the mammalian or *Xenopus* system (12,15). Furthermore, the Arg-based signal present in the GB1 receptor subunit (16) behaves as a peptide sorting motif in yeast like in mammalian cells (Figures 2 and 3). This parallel behavior suggests that Arg-based signals may be active in membrane proteins endogenous to *S. cerevisiae*. Because of their position independence within the cytosolic domains of a membrane protein (2), numerous putative Arg-based signals exist in various yeast membrane proteins. Our results suggest that some of these motifs contribute to the sorting of the respective membrane proteins and motivate further investigation of putative Arg-based signals in yeast membrane proteins.

Evolutionary conservation between yeast and mammals in the behavior of membrane proteins exposing an Arg-based signal extends beyond ER localization activity of the signal to the 14-3-3-dependent forward trafficking of multimeric membrane proteins (Figures 4–7). The challenge of manipulating 14-3-3 proteins in mammalian systems is daunting because of the high abundance of these proteins and the presence of multiple isoforms in most cell types. Thus, the Pmp2p reporter system represents a clear asset for studying the involvement of 14-3-3 in the trafficking of multimeric membrane proteins. We employed a *△bmh1△bmh2* double deletion strain to assess the combined contribution of all cellular 14-3-3 proteins to the forward transport of Pmp2p-cc-LRKR. Whilst forward transport was clearly impaired, (Figure 6) significant amounts of the reporter reached the vacuole. This leak was more pronounced than observed in the *△bmh1* deletion strain (background BY4741; Figure 7A) where the reporter localized predominantly to the ER. It is unknown why the double deletion is not lethal in the context of the Σ1278 background (28). The ER localization of the monomeric reporter Pmp2p-LRKR and forward transport of the corresponding Pmp2p-LKKK variant appeared normal (Figure S2) but we cannot exclude

that the observed leak is part of the double deletion phenotype. Since robust ER localization of Pmp2p-cc-LRKR is a phenotype of the △*bmh1* deletion strain, we believe that ER localization of Pmp2p-cc-LRKR in the △*bmh1*△*bmh2* double deletion strain to be caused by the absence of Bmh1p.

The biological significance of 14-3-3 isoforms is a major challenge in understanding the function of these highly promiscuous proteins. Examples for 14-3-3-isoform specificity in cellular processes are rare but for one mammalian isoform, 14-3-3 sigma (7). Often this is taken to mean that most isoforms are interchangeable in their biological function. There is evidence for the differential localization of 14-3-3 isoforms based on the fluorescence pattern obtained from 14-3-3-GFP fusion proteins in plant cells (5). Despite the fact that both yeast 14-3-3 proteins can bind the tetrameric form of the Kir6.2 tail, our results

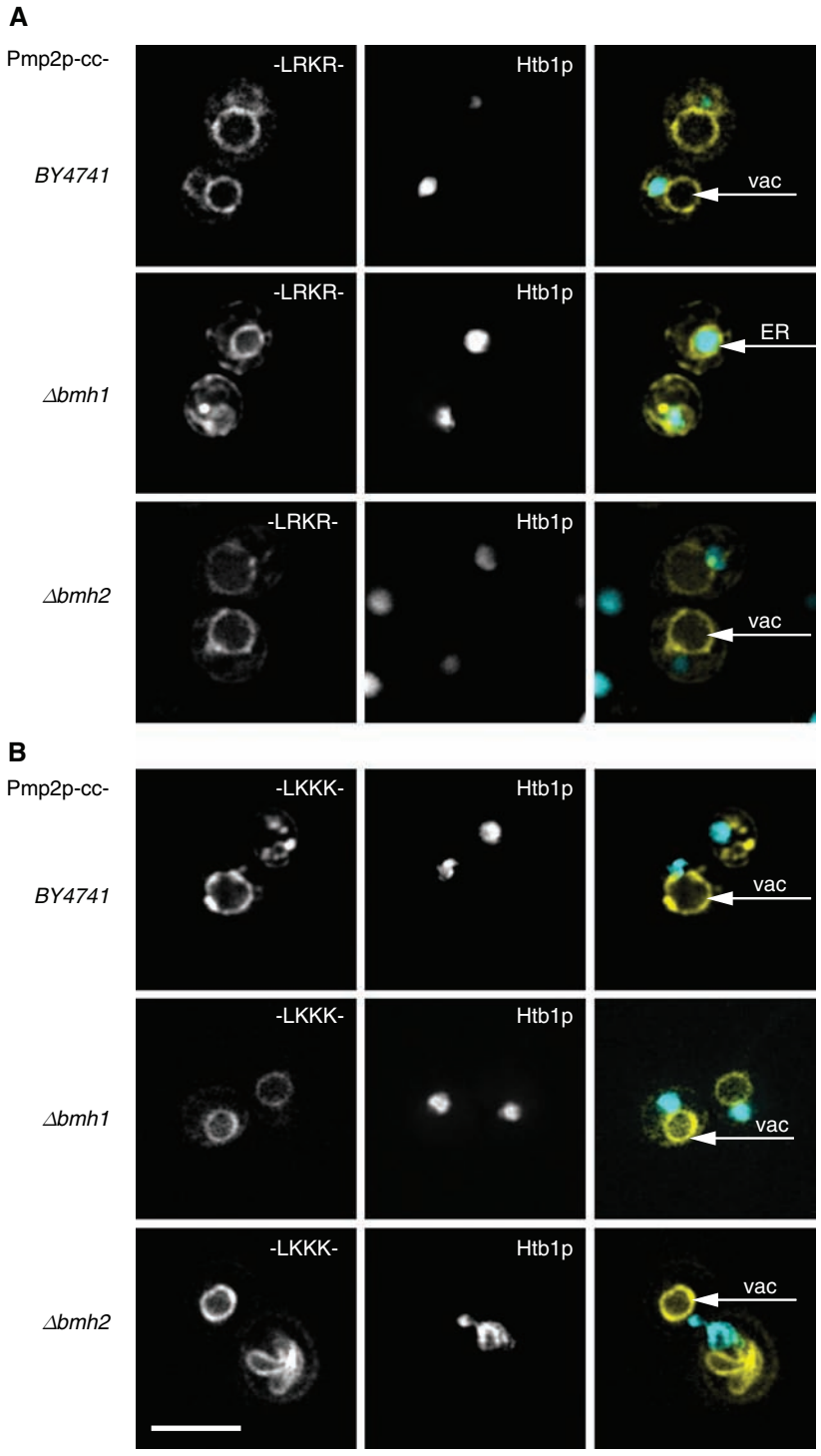

Figure 7: Loss of Bmh1p accounts for the phenotype observed in the double deletion strain. (A) Live cells of the indicated genetic background (BY4741 or derivatives; Table 1) expressing the indicated tetrameric Pmp2p-YFP fusion reporter with an active Arg-based signal from a *CEN* plasmid and a CFP fusion of histone 2B, *HTB1* (that had been integrated into the genome of the corresponding strain) were viewed under a fluorescence microscope. Image stacks were processed by volume deconvolution. YFP fluorescence images (left) are paired with the corresponding field in the CFP fluorescence channel (middle). Overlays are shown to the right (scale bar, 5 μm). White arrows indicate the perinuclear ER (ER) or the vacuole (vac). (B) Details as described in (A) for the the tetrameric Pmp2p-YFP fusion reporter with an inactive Arg-based signal to demonstrate efficient forward trafficking in the three genetic backgrounds investigated.

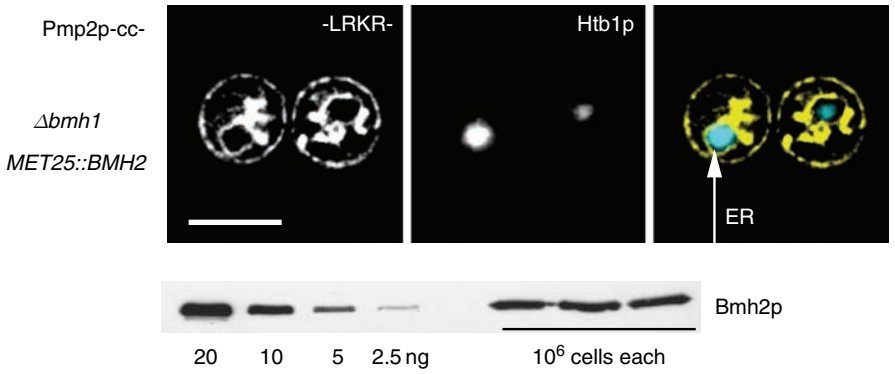

Figure 8: Increasing the copy number of Bmh2p to a similar total 14-3-3 pool as in wildtype cells does not rescue the forward trafficking defect of the Δ*bmh1* strain. *BMH2* was integrated into the genome of the Δ*bmh1* strain under the control of the *MET25* promoter. Details of the microscopy as described for Figure 7A (scale bar, 5 μm). Representative Western blot used for quantification of Bmh2p in the indicated genetic background. See text for the corresponding statistics.

reveal surprising isoform specificity in the ability of 14-3-3 to promote forward trafficking of the tetrameric Pmp2p-cc-LRKR reporter. Only Bmh1p was able to influence trafficking of the multimeric membrane protein *in vivo* while Bmh2p seemed to counteract this process (Figure 7A).

We tested alternative explanations for the specific role of Bmh1p. First, the two isoforms are present in different copy numbers with Bmh1p constituting 70–75% of the total cellular pool. This explanation is excluded by the overexpression experiment (Figure 8) in which we raised the copy numbers of Bmh2p to a number approximating the total cellular 14-3-3 content of the wildtype strain in the absence of Bmh1p: Bmh2p was not capable of promoting forward trafficking of the tetrameric Pmp2p-cc-LRKR reporter, even when present at high copy numbers. A second explanation could be based on quantitative differences in the affinity of either isoform for the tetrameric LRKR-containing tail that may not be accessible to qualitative analysis as achieved by coimmunoprecipitation (Figure 5). Quantitative determination of the respective dissociation constants (Figure 9) showed, however, that there is no significant difference in this parameter to explain the distinct effect observed *in vivo*. The concept that differential binding of Bmh1p and Bmh2p to Pmp2p-cc-LRKR cannot explain their different functional roles, is further supported by the subtle difference observed between the wt and the △*bmh2* strain for the trafficking of the tetrameric Pmp2p-cc-LRKR reporter in Figure 7A. Vacuolar sorting was actually more robust in the absence of Bmh2p than in the presence of both isoforms. This observation is consistent with a dominant negative effect of Bmh2p on the action of Bmh1p in forward trafficking to the vacuole. Our data provides mechanistic insight into the action of 14-3-3 proteins in the forward transport of a multimeric protein presenting the tail of Kir6.2: the simplest assumption, e.g. the idea that 14-3-3 proteins do nothing but shield the Arg-based signal from COPI by blocking the binding site, is not compatible with the fact that Bmh2p binds to the tetrameric tail with high affinity but cannot support forward trafficking. Thus, it seems possible that additional machinery is recruited to the membrane protein as a consequence of 14-3-3 binding and that the capacity to recruit this machinery depends on the isoform. In their structural analysis of plant 14-3-3 proteins, Sehnke *et al.* point out that variable, surface-exposed loops and the divergent C-termini may underlie isoform-specific behavior (6). These regions of the proteins may engage in isoform-specific protein–protein interactions. In general, not much is known about isoform-specific effects of the 14-3-3 proteins in yeast. Interestingly, *BMH2* was shown to rescue inviable strains with mutations in the clathrin heavy-chain gene more efficiently than *BMH1* (28,29). Since we find that only *BMH1* is capable of supporting forward transport of the Pmp2p-cc-LRKR reporter, each isoform seems to be involved in distinct processes in addition to interchangeable functions suggested by the viability of either single deletion strain. Further investigation of the isoform-specific roles of Bmh1p in forward transport will provide interesting insights into the structural principles underlying 14-3-3 isoform specificity and into the trafficking of multimeric membrane proteins.

Materials and Methods

Yeast strains and media

All *S. cerevisiae* strains used in this study are described in Table 1. Standard yeast media and genetic manipulations were as described (30). To obtain adequate expression levels from plasmids containing the *MET25* promoter cells were grown in presence of 130 μM methionine.

Molecular biology

Standard molecular biology protocols were adapted from (30) and plasmids used in this study are listed in Table 2. *PMP2* fusions to fluorescent proteins (XFP) were constructed in p415*MET25* or p416*MET25* (31) using the polymerase chain reaction (PCR). To this end, the open reading frame (ORF) of *PMP2* was amplified from yeast genomic DNA as a fragment containing a BamHI restriction site at the 5′- and a NotI site at the 3′-end, XFP ORFs were amplified adding a NotI-site to the 5′- and a Bsp120I site to the 3′-end, signal containing tails (the last 36 amino acids of the Kir6.2 protein, the last 10 amino acids of Wbp1p, and C-terminal amino acids 860–961 of the $GABA_B$ receptor subunit GB1) were fused employing a NotI

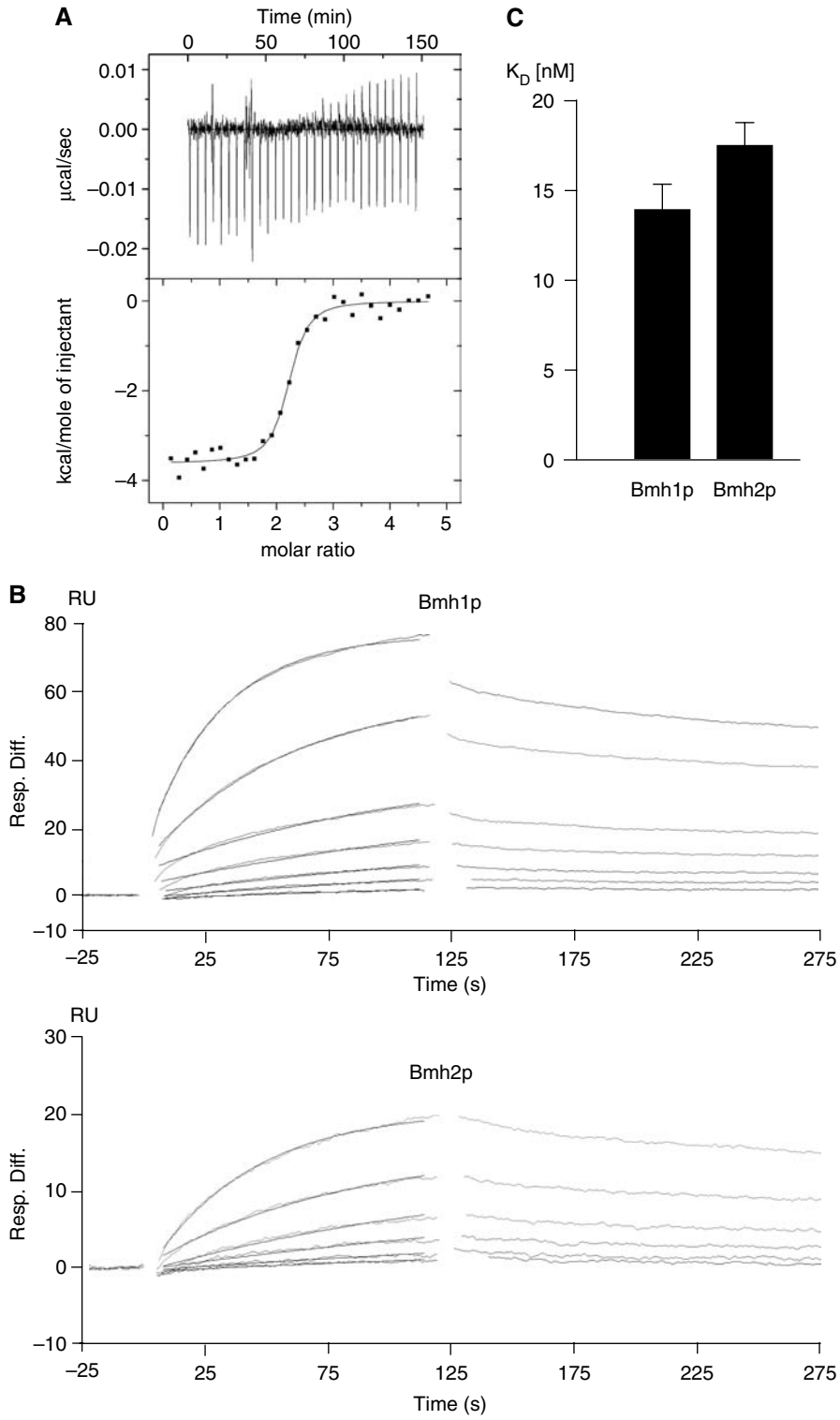

Figure 9: Quantitative characterization of the binding parameters between the tetrameric Kir6.2 tail and the yeast 14-3-3 proteins. (A) Binding curve obtained by isothermal titration calorimetry for Bmh2p isoform binding to the tetrameric Kir6.2 tail fusion protein. (B) Representative binding curves obtained by surface plasmon resonance for either isoform binding to the tetrameric Kir6.2 tail fusion protein. Curves for 14-3-3 protein concentrations from 11.7 to 750 nM and a global fit for the association phase are shown. (C) Bar graphs summarizing the dissociation constants determined by fitting the surface plasmon resonance experiments.

site (12), and the portion encoding the coiled-coil forming domain (-cc-) pLI was fused employing a Bsp120I and NotI site, respectively (3). The following primers were used in the PCR: PMP2-F (5′-cgcggatccaccatgttgatgagcacgttacc-3′); PMP2-R (5′-ataagaatgcggccgcgaatctttgtaaacctctttg-3′); XFP-Bsp120I-R (5′-ataagagggccccccttgtacagctcgtccatg-3′); cc-F (5′-cgggggcccaagaattcggcggtggatccgg-3′). All constructs were verified by sequencing. The coding region of the *HTB1* gene lacking the first 7 codons was amplified by PCR from yeast genomic DNA with primers P213 (5′-cacacaggatccgaaaccagcctccaaagcc-3′) and P214 (5′-ctctctctcgaggaccagcaccagcaccagcaccagcaccagcaccagctgcttgagtagaggaagagtac-3′). A 15 amino acid spacer was introduced with the reverse primer between *HTB1* and CFP. The PCR-product was cloned into the pCR-Blunt II-TOPO (Invitrogen, Carlsbad, CA, USA) vector, cut out with EcoRI and XhoI and cloned into the respective sites of pPS1890 (32). The 3.2 kb FspI-fragment

Table 1: Strains

S. cerevisiae strains	Genotype or characteristics	Source
Y00000	BY4741, *MATa, his3Δ1, leu2Δ0, met15Δ0, ura3Δ0*	EUROSCARF
Y06173 Δ*bmh1*	BY4741, *MATa, his3Δ1, leu2Δ0, met15Δ0, ura3Δ0, YER177w::kanMX4*	EUROSCARF
Y04034 Δ*bmh2*	BY4741, *MATa, his3Δ1, leu2Δ0, met15Δ0, ura3Δ0, YDR099w::kanMX4*	EUROSCARF
RRY1045	Sigma1278b, *MATa/alpha, ura3–52, his3::hisG, RED1+ , TRP1+/trp1::hisG, LEU2+/leu2::hisG*	Fink lab
RRY1249	Sigma1278b, *MATalpha, ura3–52, leu2::hisG, his3::hisG, bmh2::HIS3+ , bmh1::HIS3+*	Fink lab

of the resulting plasmid (pSF238) was ligated to the 2.7 kb FspI-fragment of pRS303 (33) to yield pSF273. For recombination into the yeast genome, the plasmid was linearized with EcoRV.

Expression and purification of proteins from E. coli

DH5alpha strains were used to over-express recombinant Bmh1p and Bmh2p. A tetrameric fusion protein of the last 36 amino acids of Kir6.2 to protein A-pLI (3) was immobilized on IgG Sepharose to obtain a 14-3-3-specific affinity column used for the purification of untagged Bmh1p and Bmh2p. Cells were lysed in column buffer (20 mM Tris-HCl, 50 mM NaCl, 1 mM EDTA, pH 7.4). The lysate was fractionated by a two-step ammonium sulfate precipitation (first step: 40%, second step: 70% ammonium sulfate) and 14-3-3 proteins were recovered in the ammonium sulfate precipitate of the second step, which was resuspended in and dialyzed against column buffer and loaded on the column. After extensive washing of the column with column buffer the 14-3-3 protein was eluted with elution buffer (50 mM Tris-HCl, 1.5 M $MgCl_2$, pH 7.5). The purified protein was dialyzed extensively against the buffers used in either the surface plasmon resonance or isothermal titration experiments.

Surface plasmon resonance measurements

Surface plasmon resonance experiments were performed on a BIAcore-3000 (Biacore, Uppsala, Sweden). Immobilization of a protein A-cc-LRKR fusion protein (with the tetramer-forming coiled-coil domain pLI denoted -cc-) to the CM5 Chip (Biacore) was performed using the N-hydroxy-succinimide/N-ethyl-N´-(3-dimethylaminopropyl)carbodiimide hydrochloride (NHS/EDC) method. 650 RU of the tetrameric fusion protein were immobilized. Purified Bmh1p and Bmh2p were dialyzed overnight against 10 mM Hepes, 150 mM NaCl, 50 μM EDTA, 0.005% (w/v) Tween-20, at pH 7.4. Measurements in this buffer took place at a flow-rate of 20 μL/min at 25 °C. The reference flow-cell was exposed to the same coupling procedure in the absence of any fusion protein. The chip was regenerated in a 1.5 M $MgCl_2$ solution. The binding parameters were analyzed with the BIAevaluate 3.0 software (Biacore) using the 1 : 1 binding (Langmuir) fitting protocol under the assumption that 14-3-3 proteins were present in the dimeric form. Consistent with this assumption both the purified 14-3-3 proteins migrated as dimers when subjected to Blue Native gel electrophoresis. Blue Native polyacrylamide gel electrophoresis (PAGE) analysis was performed as described by Schägger and von Jagow (34) using bovine serum albumin (BSA) as a standard.

Table 2: Plasmids

Plasmid	Description	Source
pM631	*MET25-BMH2-CYC1* fragment (subcloned in p416*MET25*) SacI/KpnI in pRS306	This study
pJ486	*BMH1* in pQE80	Görlich lab
pJ487	*BMH2* in pQE80	Görlich lab
pJ478	ZZ-cc-LRKRS- in pQE60	Schwappach lab
pJ479	ZZ-cc-LKKKS- in pQE60	Schwappach lab
pL569	*PMP2*-GFP-LRKRS- in p416	This study
pL570	*PMP2*-GFP-AAAAS- in p416	This study
pL583	*PMP2*-GFP-ARKRS- in p416	This study
pL585	*PMP2*-GFP-LRRRS- in p416	This study
pL584	*PMP2*-GFP-LRKRA- in p416	This study
pL588	*PMP2*-GFP-LRERS- in p416	This study
pL587	*PMP2*-GFP-LRIRS- in p416	This study
pL586	*PMP2*-GFP-LKKKS- in p416	This study
pM650	*PMP2*-YFP-LRKRS- in p416	This study
pM643	*PMP2*-YFP-LKKKS- in p416	This study
pN654	*PMP2*-YFP-KKXX in p416	This study
pN655	*PMP2*-YFP-AAXX in p416	This study
pN656	*PMP2*-YFP-GB1-RSRR- in p416	This study
pN657	*PMP2*-YFP-GB1-NSNN- in p416	This study
pL573	*PMP2*-cc-GFP-LRKRS- in p416	This study
pL580	*PMP2*-cc-GFP-LKKKS- in p416	This study
pL575	*PMP2*-cc-GFP-KKXX in p416	This study
pL576	*PMP2*-cc-GFP-AAXX in p416	This study
pM628	*PMP2*-cc-YFP-LRKRS- in p416	This study
pM630	*PMP2*-cc-YFP-LRKRS- in p415	This study
pM629	*PMP2*-cc-YFP-LKKKS- in p416	This study
pSF273	*HTB1*-CFP NUF-3´ UTR in pRS303	This study

Isothermal titration calorimetry

Isothermal titration calorimetry experiments were performed on a VP-ITC calorimeter (MicroCal, Northhampton, MA, USA) at 15 °C. Concentrated samples were dialyzed twice at room temperature against the same batch of 150 mM NaCl, 10 mM Hepes, at pH 7.4, 0.5 μM EDTA. After dialysis, appropriate dilutions were made using protein concentrations determined by the method of Edelhoch (35). Prior to titrations, samples were degassed for 5 min. Data were processed with the MicroCal Origin 7.0 software using the concentrations of 14-3-3 dimer, Kir6.2 tetramer (protein A-cc-LRKR) and Kir6.2 monomer (protein A-LRKR).

Western blot analysis and quantification

Yeast extracts were prepared from 10^6 log-phase cells (collected using a FACSAria cell sorter; Becton Dickinson, San Jose, CA, USA) by alkaline lysis and subsequent precipitation by trichloro-acetic acid. Extracts and defined amounts of purified protein were separated by SDS-PAGE using 10% acrylamid gels and transferred to nitrocellulose. Western Blots were blocked in TBS containing 5% milk powder and 0.02% NP-40. Primary antibodies (anti-Bmh1p rabbit 1 : 1000, anti-Kir6.2-tail guinea pig 1 : 1000, anti-Sec61p rabbit 1 : 7500) and secondary antibodies (HRP-conjugated anti-guinea pig and anti-rabbit 1 : 3000; Jackson ImmunoResearch, Soham, Cambridgeshire, UK) were diluted in blocking solution. Washes were in blocking solution and then in TBS, 0.02% NP-40. Detection was performed using the ECL system (Amersham Biosciences Europe, Freiburg, Germany). For quantification, the Western Blots were scanned and intensities analyzed with ImageJ and the Multi Measure plug-in (Rasband, W.S., ImageJ, U.S. National Institutes of Health, Bethesda, Maryland, USA, http://rsb.info.nih.gov/ij/, 1997–2005).

Subcellular fractionation on sucrose gradients

Separation of a fraction containing the ER and the vacuole from the PM was performed as described by R. Serrano (14). Logarithmically growing cells were harvested and washed once in 20 mM Hepes, 20 mM NaF and 20 mM NaN_3. Lysed with glass beads in 25 mM Tris at pH 8, 2.5 mM EDTA, Complete (Roche Applied Science, Mannheim, Germany). The lysates were cleared from broken cells by centrifugation (1200 × *g* for 2 min) and subjected to differential centrifugation at 20 000 × *g* for 20 min in a TLA45 rotor. Pellets were then resuspended in 0.55 mL of 20% glycerol in Tris-Buffer (10 mM Tris, at pH 7.4, 0.2 mM EDTA, 0.2 mM DTT) and 0.5 mL was loaded on top of a sucrose step gradient (0.5 mL 53%, 1 mL 43% in Tris buffer). After centrifugation at 100 000 × *g*/2 h in a TLS55 rotor six fractions were collected from the top and diluted 1 : 2 with 20% trichloro-acetic acid. The precipitate was washed once with ice-cold acetone and the pellets were dried at 37 °C. Samples were analyzed by SDS-PAGE and Western blotting.

Immunoprecipitation

Yeast cells were transformed with either monomeric or tetrameric Pmp2p-derived constructs. Logarithmically growing yeast cells were harvested and washed once in H_2O. Then, 500 μL glass beads and 1 mL solubilization buffer (50 mM Hepes, at pH 7.2, 100 mM NaCl, 1% Triton X-100, 0.1% SDS, 1 mM PMSF, 1 × Complete protease inhibitor cocktail Roche Applied Science) were added to a yeast pellet of 200 μL. Total yeast extract was prepared by vortexing two times for 5 min with glass beads. The lysate was cleared from unbroken cells by centrifugation (2 min, 380 × *g*). The supernatant was transferred to a new tube and cleared once more. From the supernatant, 600 μL yeast lysate with solubilized membranes (4.5 mg/mL protein) was added to 5 μL beads with immobilized anti-GFP antibody. To avoid cross-reaction of the antibodies on the Western blot, rabbit anti-GFP antibody was cross-linked to aldehyde-activated gel beads (Seize primary immunoprecipitation kit; Pierce Biotechnology, Rockford, IL, USA; 2 μg purified antibody/μL gel used for crosslink). Beads were incubated with yeast extract overnight at 4 °C, washed three times with solubilization buffer and eluted with ImmunoPure IgG elution buffer (Pierce Biotechnology). Immunoprecipitates were separated by SDS-PAGE on 10% gels and transferred to nitrocellulose for Western blotting.

Fluorescence microscopy

Microscopy was performed using a Leica DM IRE2 microscope with a Leica (Leica Microsystems, Wetzlar, Germany) 100x/1.4–0.7 HCX PL APO CS oil immersion objective controlled by OpenLab software (Improvision, Coventry, UK). Images were captured by a Hamamatsu Orca-ER CCD camera (Hamamatsu Phototonics, Herrsching am Ammersee, Germany) with excitation at 470/40 nm and emission at 525/50 nm (GFP) or excitation at 436/20 nm and emission at 480/40 nm (CFP) or excitation at 510/20 nm and emission at 560/40 nm (YFP). Where indicated the OpenLab Volume Deconvolution module was used to deconvolve z-axis images 0.2 μm apart.GFP images were processed using Adobe Photoshop (Adobe, San Jose, CA, USA); YFP and CFP images were processed by ImageJ and the corresponding Color-Merge plug-in. All images shown are representative of several independent experiments evaluated in double-blind sessions by at least two authors independently.ER-Tracker Blue-White DPX (Invitrogen) was added to the medium to a final concentration of 10 μM for 20 min at 30°C (20). Cells were sedimented, washed once with an excess of medium, and imaged using a CFP filter (480/40 nm).

Acknowledgments

We would like to thank G. Fink, D. Görlich, D. Kentner, J. Mingot, M. Seedorf, V. Sourjik and H. Yuan for the kind gift of anti-bodies, plasmids, purified protein and yeast strains. We are particularly grateful to P. van Heusden for sharing his anti-Bmh1p antiserum. J. Metz is acknowledged for excellent technical assistance and J. Lenz for FACS sorting of yeast cells on a FACSAria sorter funded by the DFG (Deutsche Forschungsgemeinschaft) and the Dietmar Hopp Stiftung. We thank members of the Schwappach lab and Matthias Seedorf for important and tremendously helpful discussions and comments on the manuscript. This research was supported by the DFG (SFB 638) and the Landesstiftung Baden-Württemberg. B.S. is the recipient of an EMBO Young Investigator Award.

Supplementary Material

Figure S1. Quantification of Bmh1p and Bmh2p in different genetic backgrounds. (A) Purified untagged yeast 14-3-3 proteins purified from *E. coli* employing a Kir6.2 affinity column. 3 μg protein of each isoform was loaded before and after the dialysis required for the surface plasmon resonance experiments. After SDS-PAGE gel electrophoresis the gel was stained by Coomassie blue. (B) Both proteins are present in the dimeric form. 5 μg of the purified proteins were resolved by Blue Native gel electrophoresis. (C) Quantification of Bmh1p. Typical Western blots used for quantitation are shown. Defined amounts of the purified proteins were resolved on 10% SDS-PAGE gels, blotted and detected using an anti-Bmh2p antiserum (23). The intensity of the bands was analyzed by image analysis and the integrated density was plotted against the protein amount loaded to obtain a calibration curve. Black diamonds represent the data points used for the linear regression curve. Open symbols represent integrated densities obtained by resolving the total protein isolated from 10^6 yeast cells of the indicated genetic background. The blots correspond to one of several similar experiments. See text for corresponding statistics. (D) Quantification of Bmh2p. Details as in (C).

Figure S2. Trafficking of monomeric Pmp2p exposing an active or inactive Arg-based signal and of tetrameric Pmp2p-cc-LKKK exposing an inactive Arg-based signal is not affected by the △*bmh1*△*bmh2* double deletion. Details of microscopy as described for Figure 2 (scale bar, 5 μm).

References

1. Ellgaard L, Helenius A. Quality control in the endoplasmic reticulum. Nat Rev Mol Cell Biol 2003;4:181–191.
2. Michelsen K, Yuan H, Schwappach B. Hide and run. Arginine-based endoplasmic-reticulum-sorting motifs in the assembly of heteromultimeric membrane proteins. EMBO Rep 2005;6:717–722.
3. Yuan H, Michelsen K, Schwappach B. 14-3-3 dimers probe the assembly status of multimeric membrane proteins. Curr Biol 2003;13:638–646.
4. Brock C, Boudier L, Maurel D, Blahos J, Pin JP. Assembly-dependent surface targeting of the heterodimeric GABAB Receptor is controlled by COPI but not 14-3-3. Mol Biol Cell 2005;16:5572–5578.
5. Paul AL, Sehnke PC, Ferl RJ. Isoform-specific subcellular localization among 14-3-3 proteins in Arabidopsis seems to be driven by client interactions. Mol Biol Cell 2005;16:1735–1743.
6. Sehnke PC, Laughner B, Cardasis H, Powell D, Ferl RJ. Exposed loop domains of complexed 14-3-3 proteins contribute to structural diversity and functional specificity. Plant Physiol 2006;140:647–660.
7. Wilker EW, Grant RA, Artim SC, Yaffe MB. A structural basis for 14-3-3 sigma functional specificity. J Biol Chem 2005;280:18891–18898.
8. Nufer O, Hauri HP. ER export: call 14-3-3. Curr Biol 2003;13:R391–R393.
9. O'Kelly I, Butler MH, Zilberberg N, Goldstein SA. Forward transport: 14-3-3 binding overcomes retention in endoplasmic reticulum by dibasic signals. Cell 2002;111:577–588.
10. Rajan S, Preisig-Muller R, Wischmeyer E, Nehring R, Hanley PJ, Renigunta V, Musset B, Schlichthorl G, Derst C, Karschin A, Daut J. Interaction with 14-3-3 proteins promotes functional expression of the potassium channels TASK-1 and TASK-3. J Physiol 2002;545:13–26.
11. Navarre C, Catty P, Leterme S, Dietrich F, Goffeau A. Two distinct genes encode small isoproteolipids affecting plasma membrane H(+)-ATPase activity of Saccharomyces cerevisiae. J Biol Chem 1994;269:21262–21268.
12. Zerangue N, Schwappach B, Jan YN, Jan LY. A new ER trafficking signal regulates the subunit stoichiometry of plasma membrane K(ATP) channels. Neuron 1999;22:537–548.
13. Nilsson T, Jackson M, Peterson PA. Short cytoplasmic sequences serve as retention signals for transmembrane proteins in the endoplasmic reticulum. Cell 1989;58:707–718.
14. Serrano R. H+-ATPase from plasma membranes of Saccharomyces cerevisiae and Avena sativa roots: purification and reconstitution. Methods Enzymol 1988;157:533–544.
15. Zerangue N, Malan MJ, Fried SR, Dazin PF, Jan YN, Jan LY, Schwappach B. Analysis of endoplasmic reticulum trafficking signals by combinatorial screening in mammalian cells. Proc Natl Acad Sci USA 2001;98:2431–2436.
16. Margeta-Mitrovic M, Jan YN, Jan LY. A trafficking checkpoint controls GABA(B) receptor heterodimerization. Neuron 2000;27:97–106.
17. Roberts RL, Mosch HU, Fink GR. 14-3-3 proteins are essential for RAS/MAPK cascade signaling during pseudohyphal development in S. Cerevisiae. Cell 1997;89:1055–1065.
18. Harbury PB, Zhang T, Kim PS, Alber T. A switch between two-, three-, and four-stranded coiled coils in GCN4 leucine zipper mutants. Science 1993;262:1401–1407.
19. Nothwehr SF, Stevens TH. Sorting of membrane proteins in the yeast secretory pathway. J Biol Chem 1994;269:10185–10188.
20. Cole L, Davies D, Hyde GJ, Ashford AE. ER-Tracker dye and BODIPY-brefeldin A differentiate the endoplasmic reticulum and Golgi bodies from the tubular-vacuole system in living hyphae of Pisolithus tinctorius. J Microsc 2000;197:239–249.
21. Winzeler EA, Shoemaker DD, Astromoff A, Liang H, Anderson K, Andre B, Bangham R, Benito R, Boeke JD, Bussey H, Chu AM, Connelly C, Davis K, Dietrich F, Dow SW *et al.* Functional characterization of the S. cerevisiae genome by gene deletion and parallel analysis. Science 1999;285:901–906.
22. Ghaemmaghami S, Huh WK, Bower K, Howson RW, Belle A, Dephoure N, O'Shea EK, Weissman JS. Global analysis of protein expression in yeast. Nature 2003;425:737–741.
23. van Heusden GP, Griffiths DJ, Ford JC, Chin AWTF, Schrader PA, Carr AM, Steensma HY. The 14-3-3 proteins encoded by the BMH1 and BMH2 genes are essential in the yeast Saccharomyces cerevisiae and can be replaced by a plant homologue. Eur J Biochem 1995;229:45–53.
24. Meusser B, Sommer T. Vpu-mediated degradation of CD4 reconstituted in yeast reveals mechanistic differences to cellular ER-associated protein degradation. Mol Cell 2004;14:247–258.
25. Letourneur F, Gaynor EC, Hennecke S, Demolliere C, Duden R, Emr SD, Riezman H, Cosson P. Coatomer is essential for retrieval of dilysine-tagged proteins to the endoplasmic reticulum. Cell 1994;79:1199–1207.
26. Overton MC, Blumer KJ. G-protein-coupled receptors function as oligomers in vivo. Curr Biol 2000;10:341–344.
27. Yesilaltay A, Jenness DD. Homo-oligomeric complexes of the yeast alpha-factor pheromone receptor are functional units of endocytosis. Mol Biol Cell 2000;11:2873–2884.
28. van Hemert MJ, van Heusden GP, Steensma HY. Yeast 14-3-3 proteins. Yeast 2001;18:889–895.
29. Gelperin D, Weigle J, Nelson K, Roseboom P, Irie K, Matsumoto K, Lemmon S. 14-3-3 proteins: potential roles in vesicular transport and Ras signaling in Saccharomyces cerevisiae. Proc Natl Acad Sci USA 1995;92:11539–11543.
30. Ausubel FM, Brent R, Kingston RE, Moore DD, Seidman JG, Smith JA, Struhl K. Current Protocols in Molecular Biology. New York: Published by Greene Publications, Associates and Wiley-Interscience: J. Wiley; 1997.
31. Mumberg D, Muller R, Funk M. Regulatable promoters of Saccharomyces cerevisiae: comparison of transcriptional activity and their use for heterologous expression. Nucleic Acids Res 1994;22:5767–5768.
32. Damelin M, Silver PA. Mapping interactions between nuclear transport factors in living cells reveals pathways through the nuclear pore complex. Mol Cell 2000;5:133–140.
33. Sikorski RS, Hieter P. A system of shuttle vectors and yeast host strains designed for efficient manipulation of DNA in Saccharomyces cerevisiae. Genetics 1989;122:19–27.
34. Schagger H, Cramer WA, von Jagow G. Analysis of molecular masses and oligomeric states of protein complexes by blue native electrophoresis and isolation of membrane protein complexes by two-dimensional native electrophoresis. Anal Biochem 1994;217:220–230.
35. Edelhoch H. Spectroscopic determination of tryptophan and tyrosine in proteins. Biochemistry 1967;6:1948–1954.
36. Juschke C, Ferring D, Jansen RP, Seedorf M. A novel transport pathway for a yeast plasma membrane protein encoded by a localized mRNA. Curr Biol 2004;14:406–411.